Photon-Photon Resonance Enhanced Modulation Bandwidth in CCIG lasers

Marco Vallone, Paolo Bardella, Ivo Montrosset
Dipartimento di Elettronica
Politecnico di Torino
Torino, Italy
marco.vallone@polito.it

Abstract— **The combined use of static and dynamic (FDTD) models allowed to determine the operation conditions of photon-photon resonance to increase lasers -3dB modulation bandwidth. The procedure, applied successfully to different laser structures exploiting this effect, is here applied to three-sections Coupled Cavity Injection Grating (CCIG) laser.**

Multisection lasers, modulation bandwidth, transfer matrix, FDTD.

I. INTRODUCTION

The continuous demand for high data rates in data communication systems increases the need of high speed, low cost light sources. Conventional lasers are internally limited by material properties, mainly the carrier transport time, determining a relatively low relaxation frequency. The possibility to use higher longitudinal modes, exploiting a photon-photon resonance (PPR) to obtain Extended Modulation Bandwidth (EMB) operation has been already studied both theoretically and experimentally, for DFB, DBR and in multi-section lasers such as Coupled Cavity Injection Gratings [1-5].

In this work we present a systematic procedure to find EMB condition that we applied to all the previous cases and we report here the application to a CCIG laser composed by two cavities (active and passive) separated by a grating section. The occurrence of this condition has been explored by varying the refractive index of the passive sections and evaluating the mode spacing between the lasing mode and the adjacent ones with a static model program. In this way, the conditions to obtain PPR are found exploiting the compound cavity interference effects. Successively the occurrence of these conditions for the three-sections laser has been verified using a Finite Difference Time Domain (FDTD) dynamic model [6].

II. THE MODEL

We studied the behavior of a three-section 1550 nm emitting multi-quantum wells AlGaInAs laser, made by a 100 µm active section, a 400 µm grating region with 20 cm^{-1} coupling coefficient, and a 100 µm passive cavity. The last two sections allow selecting the stationary mode positions and fine-tuning the frequency-distance of PPR from the main resonance. Both cavity terminal facets are cleaved.

A. Static Model

The static model is based on the well-known coupled modes equation relating the slow varying components of the co-propagating and contra-propagating fields in each section. Exploiting the transfer-matrix formalism, we end with a resonance condition on roundtrip gain (G=1) that allows for finding threshold lasing wavelength λ_m, the corresponding modal gain g_m and the threshold current. In this analysis refractive index changes due to dispersion and induced by gain variation are represented as in [5]. Resonance wavelengths for the other cavity modes at the laser threshold current are obtained searching for the wavelengths λ_n satisfying the roundtrip phase condition for integer n $\phi = 2n\pi$ with $n \neq m$ and $|G_n| < 1$.

B. FDTD Dynamic Model

The investigation of the dynamic properties of the device is performed using a FDTD model where all the effects introduced in the static model are considered. This model was initially used to validate the results obtained by the static model by computing the optical spectra at threshold, thus verifying the position of the modes. The dynamic model was then employed to calculate the electrical small signal modulation response of the device and the eye diagrams at different injected currents and bit frequencies.

III. MODELS RESULTS

Two conditions are required to obtain the EMB behavior: the lasing mode should be detuned respect to the reflectivity peak (detuned loading) and its distance respect to the cavity mode at the longer wavelength side should be below the Free Spectral Range (FSR). An example of solution exploiting this feature is reported in Fig. 1. The inset of the Fig. 1b reveals that the lasing mode belongs to a 3-folded solution, namely the lasing one (on the left), a central, unstable solution, and a stable competing one (on the right). This feature is due to the compound cavity [1] that allows for modes separation Δf_0 closer than the FSR.

Varying the effective index in grating (n_{grat}) and passive (n_{phase}) sections, a map for Δf_0 (n_{grat}, n_{phase}) has been built-up and it is shown in Fig. 2; the mode frequency separation below 40 GHz localizes operation conditions with possible EMB.

The research leading to these results has received funding from the European Community's Seventh Framework Programme (FP7/2007-2013) under grant agreement n°224366 (De light project).

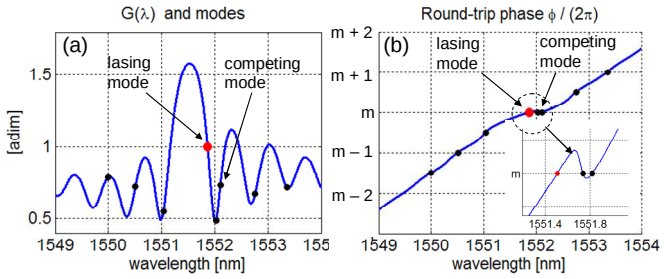

Figure.1: Example of round trip gain $|G|$ (a) and phase $\phi(G)$ (b), versus wavelength. Dots represent lasing (red) and competing (black) modes.

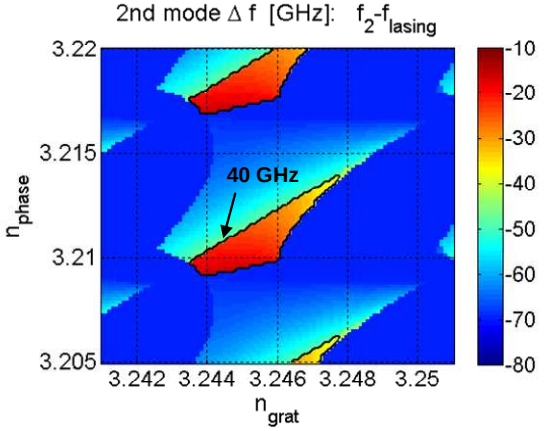

Figure 2: Frequency separation Δf_0 map in the space of effective indexes of grating and passive sections. An arrow indicates the 40 GHz contour.

Having fixed n_{phase} at 3.21 and varying n_{grat}, static and dynamic models yield the results shown in Fig. 3, where the modes position in the (n_{grat}, λ) plane is shown. EMB can take place only when a mode (blue track: static model, crosses: FDTD) is very near ($\delta\lambda$ < 0.2-0.3 nm) and on the longer wavelength side to the lasing mode (red track and circles respectively).

In order to verify the effect of PPR on CCIG modulation bandwidth, many FDTD simulations have been performed for different values of n_{grat} to calculate the small signal modulation (IM) response. This modulation map, reported in Fig. 4, shows that, for values of n_{grat} near 3.2425, in addition to the resonance peak around 8GHz, a strong peak appears at 58 GHz. This second peak is originated by PPR and its position is exactly the frequency separation between the lasing mode and its closest one. By increasing n_{grat}, the frequency distance between the modes reduces (see Fig. 3), and the gap between the relaxation oscillation peak and the PPR is also progressively reduced (A), until a 33 GHz -3dB modulation bandwidth condition is obtained (B). For an additional increase of n_{grat} (C), the two modes merge leading to the formation of a strong peak in the IM.

We finally report in Fig. 5 the eye diagrams obtained by a large signal modulation at 33GHz and 40GHz of the CCIG at the maximum EMB small signal modulation condition. The results are comparable to what presented in [3] for a DFB with feedback controlled by an integrated external cavity.

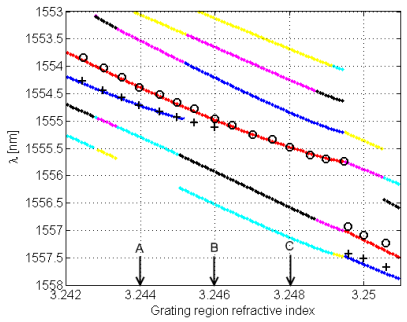

Figure 3: Modes map (static model: solid line; FTDT: circles and crosses). EMB may occurs for n_{grat} in [3.244, 3.246] range between lasing (o) and side (x) modes.

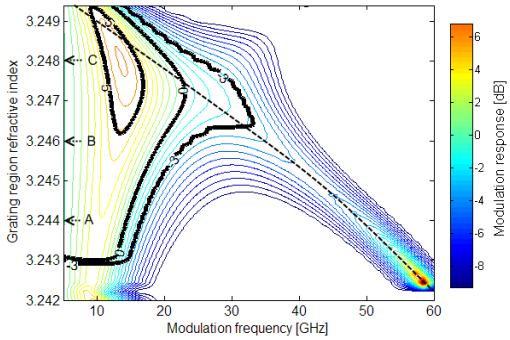

Figure 4: Map of the small signal modulation responses, calculated at 70 mA (2 I_{th}) as a function of n_{grat}. Black lines +3, 0 ,-3dB contours.

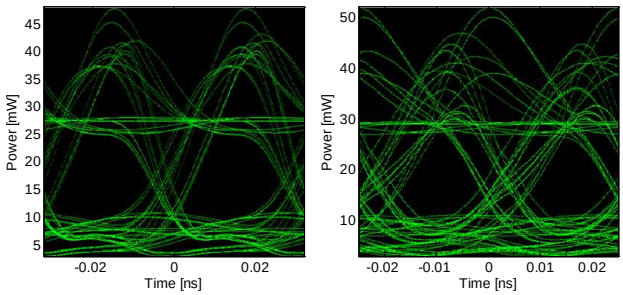

Figure 5: CCIG eye diagrams obtained by a directly current modulation between 45mA and 100mA at 33GHz (left) and 40GHz (right).

IV. Conclusions

Two complementary models have been proposed to search for EMB operation. First, a static analysis of the laser cavity modes allows finding proper PPR conditions, then with FDTW the condition for EMB is verified by computing both the small and large signal modulation responses. As an example, we reported the results obtained for a CCIG laser. A correct positioning of the cavity modes through a fine-tuning of the device parameters allowed obtaining a -3dB EMB of around 33GHz.

References

[1] G. Mortier et al., *IEEE J. Quantum Electron.*, vol. 36, n. 12, Dec. 2000.

[2] U. Feiste, *IEEE J. Quantum Electron.*, vol. 34, n. 12, Dec. 1998.

[3] M. Radziunas et al., *IEEE J. Sel. Top. Quantum Electron.*, vol. 13, 2007

[4] U. Troppenz et al., EOS Annual Meeting 2008

[5] W. Kaiser et al., *IEEE Photon. Technol. lett.*, vol. 16, n. 9, Sept. 2004.

[6] P. Bardella et al., *IEEE J. Sel. Top. Quantum Electron.*, vol. 11, 2005